Int. J. Electrochem. Sci., 8 **(2013)** 9474 - 9498

International Journal of
ELECTROCHEMICAL
SCIENCE
www.electrochemsci.org

Electric Desalting and Dewatering of Crude Oil Emulsion Based on Schiff Base Polymers As Demulsifier

Ayman M. Atta

Chemistry Department, College of Science, King Saud University, P.O.Box - 2455, Riyadh - 11451, Kingdom of Saudi Arabia
E-mail: aatta@ksu.edu.sa

Received: 8 May 2013 / *Accepted:* 12 June 2013 / *Published:* 1 July 2013

The effect of electric desalting on dewatering process was studied in this paper. Some surfactants are used as demulsifiers for destabilization of emulsions of crude petroleum. We have developed new Schiff base polymers for such use; their chemical structures were determined by FTIR and ^{1}H NMR. The prepared surfactants were dissolved in xylene/ethanol (75:25) and toluene (commonly employed in commercial formulations) and also in water. Surface tensions and critical micelle concentrations for water soluble surfactants were determined at several temperatures. Surface excess concentration Γ_{max} and the areas per molecule at the interface A_{min} were determined from the adsorption isotherms of the surfactants. Our surfactants have long hydrophobic segments which efficiently break down crude petroleum emulsions. The best demulsifier efficiency is seen for xylene/ethanol (75:25). The solvent mixture improves the diffusion of the molecules of the Schiff bases in the petroleum phase of the emulsion and acts as a co-additive.

Keywords: Schiff bases, polymeric surfactants, ethoxylation, demulsifiers, micellization, adsorption.

1. INTRODUCTION

Petroleum is typically produced as a water-in-oil emulsion. The water must be removed (down to a level of < 1 %) in a process usually called demulsification or dehydration which consists of forcing the coalescence of water droplets and producing their separation by settling. Water-in-oil emulsions are stabilized by a wide range of materials that appear naturally in heavy oil, such as asphaltenes, natural surfactants, and clays. Water elimination has to meet pipeline specifications) and destabilization of the emulsion is essential. Demulsification can be achieved by three means: mechanical, electrical, and chemical. The addition of chemical demulsifiers is the most widely used method [1]. An effective demulsifier is a surface-active compound that can absorb onto the water/oil interface and change its properties such that water droplets aggregate and coalesce. Attempts have been made to correlate the efficiency of demulsifiers with their surface, interfacial, and chemical properties [2 - 5]. A large number of demulsifiers have been developed and derived from surfactants [6 - 8]. Commercial demulsifiers are often polymeric surfactants such as co-polymers of polyoxyethylene (PE) and polyoxypropylene (PO) or alkylphenol-formaldehyde resins, dodecylbenzenesulphonic acid, or else blends of different surface-active compounds [9 - 11].

In our quest for new polymeric demulsifiers, we have focused on Schiff bases, condensed organic derivatives containing azomethine groups C=N-. Schiff bases have already extensive applications in several areas [12 - 14] including the petroleum field [15 - 17] and one of us has done work in this area before [14, 15]. Polymeric Schiff base ligands lead to novel structural types and display a wide variety of thermal properties [18, 19]. In this work we have synthesized a new class of soluble such Schiff bases and evaluated them as demulsifiers for crude petroleum at temperatures not exceeding 60 ^{o}C. The correlation between the surface activity of the prepared Schiff base surfactants and their performance as demulsifiers is another goal of the present work.

2. EXPERIMENTAL

2.1. Materials

Octadecyl amine (ODA), dodecyl amine (DDA), *p*-hydroxybenzaldehyde (HBA) and *p*-formaldehyde were obtained from Aldrich Chemical Co., and used without purification. *S*odium hydroxide, sulphuric acid were obtained from Elnasr Pharmaceutical Co. (Egypt). All solvents were purchased from Aldrich Chemical Co. (Germany).

Table 1. Specification of Ras Tanura Arab heavy crude oil.

Test	Method	Value
API gravity at 60^{o}F	Calculated	27.4
Viscosity at 100^{o}F (Cst)	IP71	125
Specific gravity at 60^{o}F	IP 160/87	0.891
Asphaltene contents (wt. %)	IP 143/84	8.27
Saturates (wt. %)		16.5
Aromatics (wt. %)		24.2
Resins (wt. %)		49.3
Solid content (PTB)	ASTM D381	661
Fe (ppm)		157
Ni (ppm)		2.7
V (ppm)		34
Naphthenic acid (mg KOH/g)	ASTM D664	0.3
Acid number (mg KOH/g)	ASTM D4310	7.6

Table 1 presents details of the Arab heavy crude oil (received from Ras Tanura, Saudi Arabia) and its origin. On the other hand, formation water produced from Ras Tanura was used to obtain crude oil emulsion, produced from Ras Tanura, Saudi Arabia.

2.2. Preparation of Schiff base monomer and polymer surfactants

2.2.1. Synthesis of Schiff base of monomers

The reactions were performed in a three-necked flask (0.5 L capacity) equipped with a condenser, magnetic stirrer, thermometer, dropping funnel and nitrogen atmosphere inlet. The flask was charged with ODA or DDA (0.25 mol) and 200 ml absolute ethanol. HBA (0.25 mol) was dissolved in 200 ml absolute ethanol and the solution was added into flask within 1 h with stirring in the presence of nitrogen gas. The temperature of reaction was gradually increased up to reflux for 3 h. The reaction was cooled to filtrate the solution. The products of condensation of *HBA* with ODA and *DDA* are designed as ODS and DDS, respectively.

2.2.2. Synthesis of Schiff base Polymers

The methylation of Schiff base in a melting process was carried out with the 1 mol of a Schiff base (ODS or DDS) and 3 mol of paraformaldehyde. The Schiff base was intensively mixed with *p*-formaldehyde, NaOH (1 wt. % based on the weight of reactants) and heated to 180°C under nitrogen atmosphere. After 30 min the reflux condenser was removed and the water formed was distilled using a Dean & Stark separator. After no more water could be distilled, the temperature of the reaction mixture was shortly (about 5 min) raised up to 200 °C. Then the methylated Schiff base was removed from the flask and cooled to room temperature. The yield of the yellow to amber-coloured methylol Schiff bases ranged from 85 to 90 %. The polymers so produced from ODS and DDS monomers can be designated as PODS and PDDS, respectively.

2.2.3. Ethoxylation of Schiff-Base Monomers and Polymers

A high pressure stainless steel autoclave (Parr model 4530, USA) of 1 L capacity, 400 psi maximum pressure and 180˚C maximum temperature was used for ethoxylation reaction. The autoclave is equipped with a magnetic drive stirrer, an electric heating mantle with a thermocouple inserted in the reactor body, a cooling coil, a pressure gauge and a drain valve. The prepared ODS, DDS and their polymers were charged into the reaction vessel with Na metal as a catalyst (0.3 wt. %), the reaction mixture was heated to 180˚C with continuous stirring while passing a stream of nitrogen gas through the system for 10 minutes to flush out air. The nitrogen stream was then replaced by ethylene oxide. The ethylene oxide was introduced through the inlet gas valve until the desired amount of ethylene oxide was reacted. Generally, as a result of the introduction of ethylene oxide, the pressure was substantially increased as indicated by the pressure gauge, until it reached a maximum value. The pressure drop indicates ethylene oxide consumption. The reaction completion was established when the pressure reached its minimum value. At this stage, heating was stopped and the contents was cooled gradually to ambient temperature by means of the cooling coil connected to the reactor carrying cold water. After cooling, the product obtained was discharged, weighed and neutralized with HCl. The ethoxylated products of ODS, DDS, PODS and PDDS can be designated as EODS, EDDS, EPODS and EPDDS, respectively.

2.3. Measurements

The crude oil and n-pentane (ratio 1:5) were agitated homogeneously at room temperature, and the mixture was then centrifuged (LG10-2.4A, Jingli Centrifugal Equipment Co., Ltd., Beijing, China) at 2400 rpm for 10 min to separate the asphaltenes. The extraction of the resin fraction can be divided as follows: 2 g of silanol per 1 mL crude oil was added to the supernatant liquid from the asphaltenes precipitation. The mixture was stirred homogeneously, centrifuged for 3 min at 1000 rpm, and the supernatant phase was removed. The coated particles were then mixed with benzene, stirred, and centrifuged for 2 min at 1000 rpm. Decantation and filtration were performed several times until the supernatant phase was nearly colorless after centrifugation. The desorption process was repeated using the same procedure with a blend of 7 % methanol and methylene dichloride. The resins were separated from the solvent/resin mixture after removal of solvent at 90 °C in a rotary evaporator, and this last step was performed under a nitrogen blanket to ensure that all of the solvent was removed [20]. The WC-2 microcoulometric detector of salt content was used to detect the salt content in crude petroleum.

Initially, the solubility tests were performed in different solvent media for EODS, EDDS, EPODS and EPDDS, at a concentration of 40 % (w/v), at room temperature, with toluene, xylene, ethanol, and xylene/ethanol (75:25). Then all four ethoxylated Schiff base monomers and polymers were evaluated at concentrations of 50, 100, and 250 ppm, using xylene/ethanol (75:25), and water as the solvent systems. The solubility and cloud temperature tests were performed in a test tube immersed in a beaker containing water, placed over an agitation and heating plate. The solutions containing each additive were first heated and then slowly cooled. The temperatures were determined by a thermometer placed in the test tube and ranged from 10 to 85 ^{o}C. Two duplicates were prepared of each solution, and there were two cloud point temperature readings for each solution, determined by the average between the temperature at which the first indication of clouding appeared and the temperature at which the clouding disappeared. These tests were performed by visual inspection.

The relative solubility number (RSN) values of the surfactants were measured by the newly developed method using ethylene glycol dimethyl ether and toluene as titration solvents. In this method, 1 g of surfactant was dissolved in 30 mL of solvent consisting of toluene and ethylene glycol dimethyl ether and the resultant solution was titrated with deionized water until the solution became persistently turbid. The volume of water in mL titrated in was recorded as the RSN number.

The nitrogen content was measured with a Tecator Kjeltech auto analyzer. A Tecator 1007 digester was used for the initial digestion of the samples.

Infrared spectra were determined with a Perkin-Elmer model 1720 FTIR (KBR). ^{1}H-NMR spectra of monomers and polymers were recorded on a 400MHz Bruker Avance DRX-400 spectrometer.

Molecular weights of PODS and PDDS were determined by using a Muffidetector GPCWaters 600-E model equipped with Styragel columns.

The surface tension measurements of the prepared surfactants were carried out at different molar concentrations at 25^{o}C by using a ring platinum Kruss K-10 tensiometer. All of the measurements were made in triplicate, values with variation less than 1 mN/m were included in the averages.

The salt water-oil interface tension measurements were performed by the pendant drop method [21] using a DataPhysics model OCA-20 automatic contact angle meter (goniometer), to observe the interfacial behavior of the samples as a function of time; measurements were made at 25 ^{o}C. The surfactants were dispersed in the aqueous phase (salt water), in xylene/ethanol (75:25) and in crude petroleum. Surfactant concentrations from 50 to 250 ppm were used. In pendant drop tests, a droplet is formed at the end of a straight needle (d = 0.89 mm) connected to a syringe with electronic control of the droplet, within an optical glass cuvette containing a fixed volume of the solution. The droplet is subject to interfacial tension and gravitational forces and is filmed by a camera. The measurements were taken at 1 min intervals, and the interface tension (IFT) was determined by digitalizing the images and analyzing the profile of the droplets by applying the Young -Laplace [22] equation:

$$\Delta P = (\rho_o - \rho_a)\, gh - \mathrm{IFT}\,(1/r_1) + (1/r_2) \qquad (1)$$

where ΔP is the pressure difference across the interface (inside and outside the droplet), ρ_o and ρ_a are the densities of the oil and aqueous phases, respectively, g is gravity, h is the height of the liquid column of the droplet, and r_1 and r_2 are the principal radii of curvature. The errors of these measurements are indicated in the equipment manual as not larger than 5%.

2.4. Preparation of water and crude petroleum emulsions

Water-in-oil emulsions collected in the field were free of demulsifier. Shortly after collection, samples were drained of any free water. Free water is defined as water that separates rapidly and is not emulsified. All emulsions were prepared with a total volume of 100 mL. The ratio between crude petroleum and the aqueous phase (formation water) was in the range 10- 50 vol. %. The emulsions were prepared by mixing using a Silverstone homogenizer. In a 500 ml beaker, the crude petroleum was stirred at 35^{o}C (1500 rpm for 1 h) while sea water was added gradually until the two phases become homogenous. The ratios crude oil : water were 90:10, 80:20, 70:30 and 50:50.

2.5. Electric Desalting and Analysis of Salt Content in Crude Oil.

The crude oil sample was delivered into the homogenizer after preheating and stirring uniformly, in which 10% (wt) of formation water was also added, and then stirred at 9000 r/min for 1 min. After that, the emulsion and appropriate demulsifier were put into test bottles. The bottles that are equipped with electrodes were placed fixed in the oscillator and shaken for 1 min, then stored in a constant temperature bath at 85 (2 °C for 10 min, electric field for 20 min, and allowed to settle for another 10 min. The volume of the separated water was recorded every 5 min. The salt content in oil after desalting was analyzed. A PDY-1 instrument of electric dewatering was used in the experiment and a WC-2 microcoulometric detector of salt content was used to detect the salt content in crude oil. The principle of the detector is that crude oil mixed with polar solvent was heated to extract the salt, and then centrifuged. A small amount of extracted liquid was taken out by injector and delivered into the ethanoic acid electrolyte containing amounts of silver ion, so the chlorine ion of the sample can react with the silver ion. The consumed silver ion for the reaction will be supplied by electrode, so according to Faraday's laws (of electrolysis), salt content of the sample will be obtained by measuring the changing of electric quantity for supplying silver ion.

2.6. Demulsification of the Prepared Emulsions

The bottle test is used to estimate the capability of the prepared demulsifiers in breaking of water in oil emulsions. Demulsification was studied at 45-60 ^{o}C by gravitational settling using graduated cone-shaped centrifuge tube. Our Schiff base surfactant solutions were injected in turn into the emulsion using a micropipette. After the contents in the tube had been shaken in an oscillating shaker for 1 minute, the tube was placed in a water bath at 45-60^{o}C to allow the emulsion to separate. The phase separation was recorded as a function of time. During the settling, the interface between the emulsion and separated water phase can be easily observed. The demulsification efficiency (DDE%) can be calculated from the equation; DDE %= Vox100/V1, where Vo and V1 are the volume of separated and blended formation water, respectively.

3. RESULTS AND DISCUSSION

3.1 Characteristics of the synthesized materials

A number of researchers have tried to synthesize high molecular weight poly-Schiff bases but failed due to their poor solubility in common organic solvents and the infusibility of the products [23-25] – although some soluble, film and fiber forming poly-Schiff bases were reported [14, 15, 26, 27]. Such bases can be prepared either by polycondensation of dialdehyde with diamine or by etherification with formaldehyde in acid or alkali media [19]. We have proceeded by ethoxylation of Schiff base monomers and polymers as described in the experimental section and also shown in Scheme 1. The reaction took place between p-hydroxybenzaldehyde and octadecyl amine or dodecyl amine produced 4-hydroxybenzaldehyde-*N*-octadecylimine (ODS) or 4-hydroxybenzaldehyde-*N*-octadecylimine (DDS), respectively. The polymers are dark black powders and are insoluble in benzene, toluene, and water but soluble in dimethylformamide (DMF) and acetone. Physicochemical characteristics of so prepared Schiff base monomers and polymers are listed in Table 2. PDI denotes the polydispersity index = M_w/M_n. The purity of the Schiff base monomers and polymers is very important since they are starting materials for making water-soluble Schiff base polymeric surfactants.

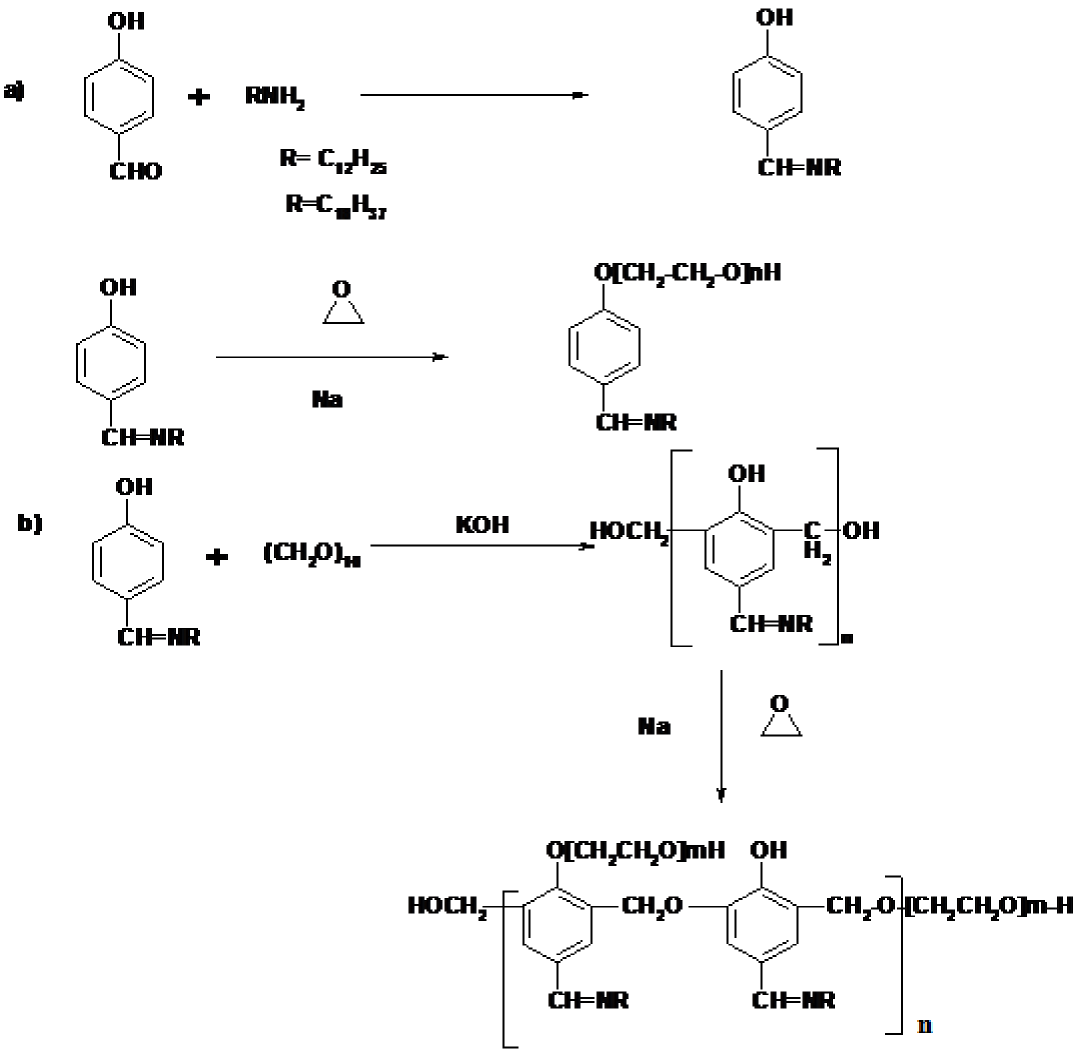

Scheme 1. Ethoxylation of Schiff base a) monomers and b) polymers.

Nitrogen content inn Table 2 indicates good agreement between the experimental and theoretical values. This means that the synthesis and purification were performed successfully. The M_n, M_w and PD values indicate successful etherification of DDS and ODS monomers with *p*-formaldehyde. The PD values are relatively low, indicating a narrow molecular weight distribution.

Solubility tests of EODS, EDDS, EPODS and EPDDS at room temperature were carried out in water, toluene, xylene, ethanol, and xylene/ethanol (75:25). Among these, toluene and xylene/ethanol (75:25) are the dispersants normally used for formulations containing demulsifying additives [28-32]. All prepared surfactants are soluble in toluene and the xylene/ethanol mixture throughout the temperature range studied (25-65 ^{o}C). As expected, EPODS and EPDDS polymers decrease their solubility in water along with the temperature increase. The reason is that their solubility is related to the hydration of the polar groups present in the molecules (the oxyethylene groups) [28]. The hydration of the oxygen atoms of ether by hydrogen bonds results from the interaction of at least two water molecules per EO unit, so that hydration increases with an increasing length of the PEO chain [33].

Table 2. Physicochemical characteristics of Schiff base monomers and polymers.

Compounds	Nitrogen content (wt. %)		GPC results			Melting Temperature (°C)	Yield (%)
	Theoretical	Determined	M_n	M_w	PDI		
ODS	3.86	3.82	-	-	-	112	90
DDS	4.86	4.81	-	-	-	128	85
PODS	3.56	3.66	5942	9400	1.58	150	75
PDDS	4.40	4.48	5204	9027	1.73	140	70

As the temperature of these systems rises, the hydrogen bonds are broken and the non-ionic surfactants lose their solubility in water. The cloud point is the temperature below which there is a single phase of a molecular solution. Above the cloud point, a non-ionic surfactant loses its solubility in water, causing the formation of two phases and giving the mixture a cloudy aspect [34]. To investigate the effect of the temperature on the solubility of the EODS, EDDS, EPODS and EPDDS in aqueous medium (up to 85 °C), the cloud points were measured at concentrations of 40, 400, and 1200 ppm. The results are shown in Table 3. As expected, when the surfactant concentration increases, the cloud point temperature decreases. EDDS and EPDDS surfactants are more soluble in water than EDDS and EPDDS. This means that the alkyl substituents are the main factor determining solubility – as in fact reported before [28, 30].

Table 3. Degree of ethoxylation and cloud temperatures of the Schiff base monomers and polymers.

surfactants	EO (%) [1]	EO (%) [2]	Number of ethylene oxide units [2]	Theoretical molecular weight M g/mol	Cloud temperature (°C) at different surcatant concentrations (ppm)		
					500	1000	5000
EODS	100	100	18	1155	75-76	77-78	80-82
EDDS	100	100	15	948	>85	>85	>85
EPODS	63.5	60	10	$12.5 \cdot 10^3$	70-71	73-75	76-77
EPDDS	58.5	55	9	$9.7 \cdot 10^2$	78-79	80-81	83-84

[1] determined from weight difference between reactants and products.
[2] determined from ^{1}H NMR analysis.

Chemical structures of our monomers and polymers and their ethoxylated derivatives were determined from FTIR and ^{1}HNMR analyses. The FTIR spectra of DDS, ODS, EPDDS and EPODS are selected as representative samples and displayed in Figure 1a-d. ^{1}H NMR spectra of EDDS, EODS, EPDDS and EPODS are shown in Figure 2a-d.

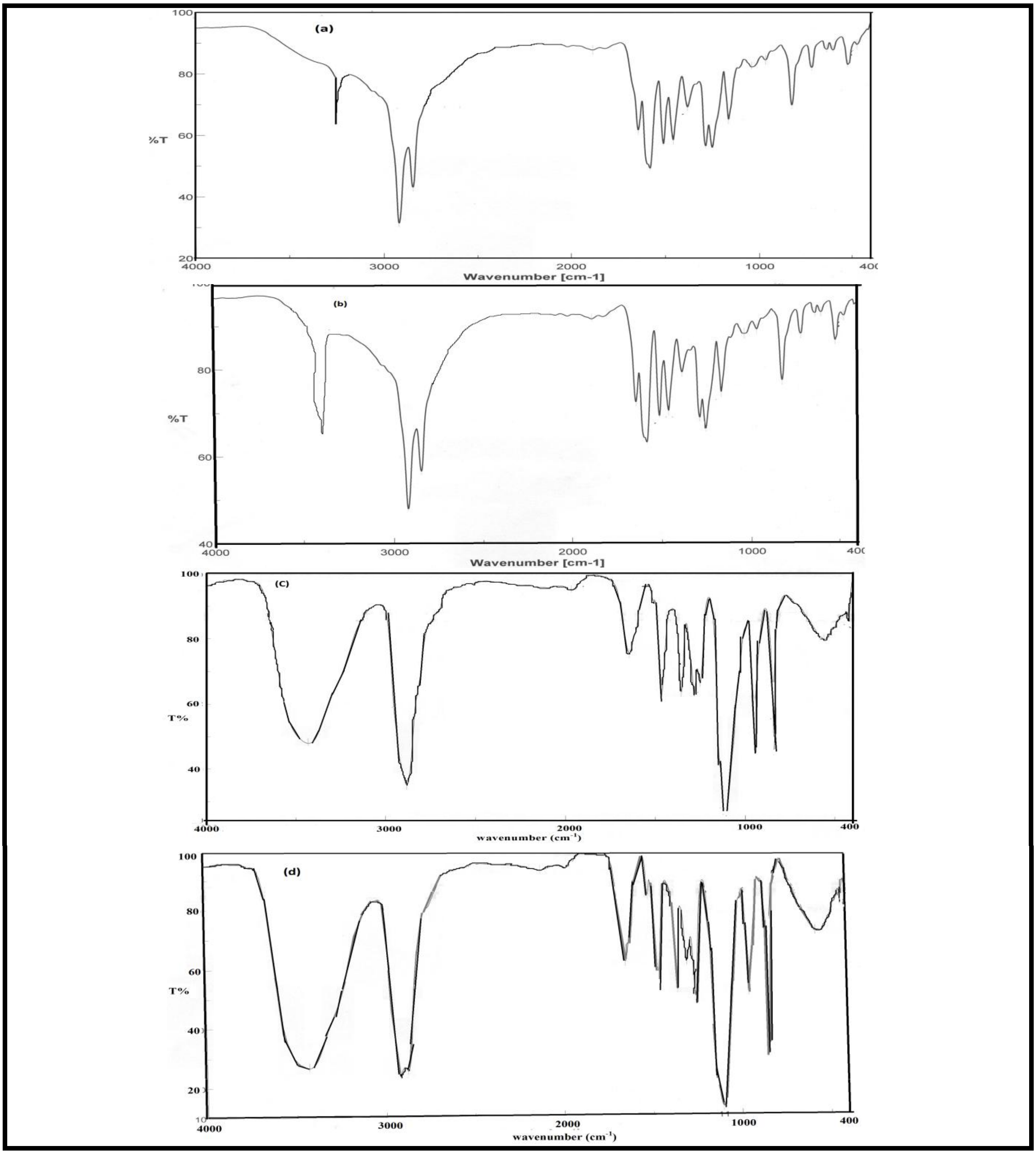

Figure 1. FTIR spectra of a) ODS, b) DDS, c) EPDDS and d) EPODS.

The FTIR spectra in Figure 1 provide valuable information on the nature of functional groups present. The lack of O–H stretching band in the 3400–3500 cm^{-1} range in the spectra of the ethoxylated derivatives confirms complete ethoxylation. There is a new strong absorption band at 800 cm^{-1} assigned to C–H out-of-plane bending – what indicates the formation of tetra substituted Schiff base polymers. The appearance of strong peaks in the spectra of both Schiff base and ethoxylated derivatives in the region 1580–1670 cm^{-1} (Figure 1a-d) indicates the presence of C=N stretching bands [35]. The disappearance of strong bands of aldehyde groups at 2750 and 1700 cm^{-1} assigned to CH and C=O stretching of aldehyde groups indicates the formation of Schiff base monomers and polymers with high purity.

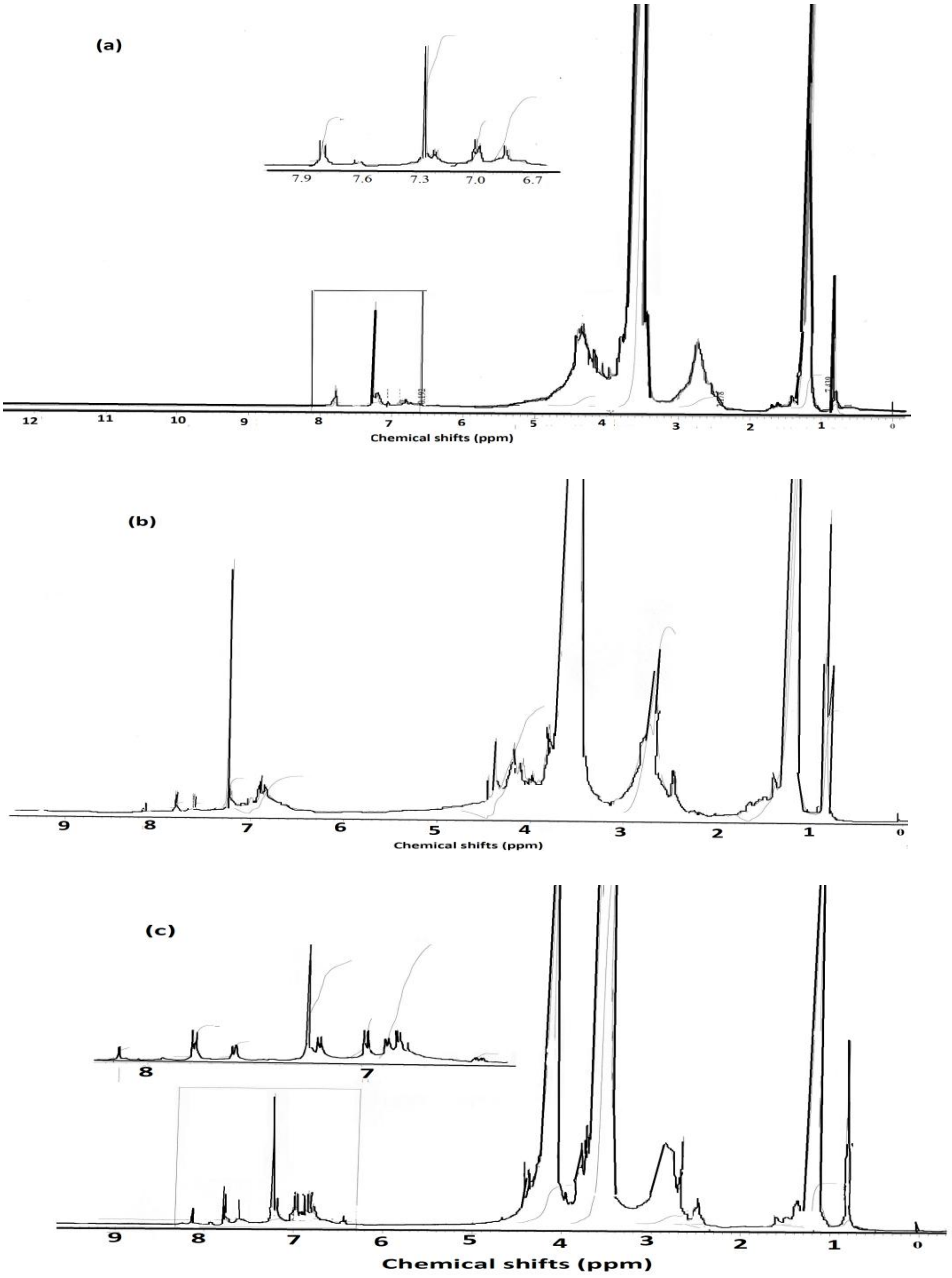

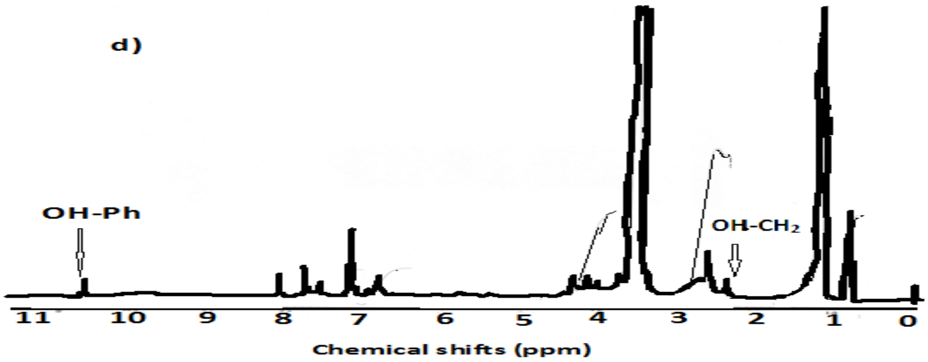

Figure 2. ^{1}H NMR spectra of a)EDDS, b)EODS, c)EPODS and d) EPDDS.

Figure 2 shows a complicated aromatic proton multiplet (7.1-7.6 ppm) and an imino proton singlet at 6.8 ppm, down from the usual aromatic proton region. The disappearance of strong band of chemical shift at 11.9 ppm assigned to OH aromatic groups of Schiff bases also indicates the ethoxylation of Schiff bases. The triplet peaks observed in spectra of EODS, EDDS, EPDDS and EPODS at 4.2 ppm can be assigned to CH_2 groups attached directly to azomethine groups. A multiple peak at 2.1 ppm (Figure 2) can be attributed to $(CH_2)_n$ of alkyl groups.

The ethoxylation of Schiff base monomers and polymers can be proven by appearance of new peaks of oxyethylene units at 3.6 ppm and -OH proton of PEG 2.5 ppm. The ^{1}H NMR spectroscopic analysis was used before for determining the propylene oxide/ethylene oxide ratio for the PPO-PEO block copolymers [36]. Here that analysis is used to determine the ethoxylation ratio or number of oxyethylene unit from integration ratio between the oxyethylene units in the hydrophilic moiety and the phenyl rings in the hydrophobic moiety, (EO/phenyl ratio) for EODS or EDDS monomers. The number of oxyethylene unit and degree of ethoxylation of EPDDS and EPODS can be determined from integration ratio between -OH of phenol (11.9 ppm) and -OH of ethoxylated units (2.5 ppm). The results are listed in Table 3. The results in Table 3 were used to calculate theoretical molecular weights of ethoxylated Schiff base monomers and polymers. The ethoxylation percentage can be also determined from weight differences between reactants and products – as displayed in Table 3. The calculated ethoxylation percentages (EO %) from ^{1}H NMR data agree with those from weight measurements. The results in Table 3 also reveal that the concentration of EO in PODS is higher than that determined for PDDS Schiff base polymers. The values are 63.5 wt. % and 58 wt. % for EPODS and EDDS, respectively. The theoretical molecular weight can be determined from number of oxyethylene units (determined from ^{1}H NMR analysis), EO concentration and the number of the repeating units for PDDS and PODS and are listed in Table 3. The molecular weight was calculated as $M = M_{ethoxylated}n_1 + M_{unehoxylated}n_2$ where n_1 and n_2 are numbers of ethoxylated and unethoxylated units. We see a higher M value for EPODS than for EPDDS.

3.2. Surface activity of the Schiff base surfactants

Virgin nonionic surfactants were reported as soluble in various solvents including water, slightly acidic water and methanol, but less soluble in basic water [37]. The polymerization and ethoxylation of ODS and DDS yield different hydrophobicity, chain flexibility and solubility due to differences of inter- and intramolecular interactions. The solubility and state of surfactant solutions should depend on the hydrophobe composition and hydrogen bonds between polar groups of modified Schiff base monomers and polymers. The difference in solubility is due to the difference in hydrophil-lipophil balance (HLB) of the surfactants. HLB is one of the most important characteristics of a surfactant. The HLB values were calculated by using general formulae for nonionic surfactants [38]:

$$\text{HLB} = \text{EO\%} / 5 \qquad (2)$$

$$\text{HLB} = [(M_H \times 20) / (M_H + M_L) \qquad (3)$$

Here M_H and M_L are molecular weights of hydrophilic and hydrophobic moieties, respectively. HLB values so calculated are listed in Table 4.

Table 4. Surface activity of the Schiff base surfactants.

designation	HLB		RSN	$(-\partial\gamma / \partial \ln c)$	c_{mc} g/L $*10^4$	γ_{cmc} mN/m	Γ_{max} x 10^{10} mol/ cm^2	A_{min} nm^2/ molecule
	Eq. (2)	Eq. (3)						
EODS	13.7	-	14	5.03	6.1	36.5	2.1	0.79
EDDS	13.9	-	18	3.97	9.2	40.1	1.7	0.97
PEODS	12.5	11.8	13	5.30	2.1	38.2	2.2	0.75
PEDDS	11.7	11.2	11	4.50	5.4	42.3	1.9	0.87

In the Table γ is the surface tension, c the solute concentration, c_{mc} the critical solute concentration, Γ_{max} is the excess surface concentration and A_{min} is the area per molecule at the interface

The solubility of nonionic surfactants in water increases with increasing HLB values. The HLB values range from 11.2 to 13.9, testifying to good solubility. Since HLB is difficult to determine experimentally, alternatively relative solubility numbers (RSNs) can be used to represent the hydrophobicity of the surfactant [38]. These results are also listed in Table 4. We find that, at a fixed EO number, the RSN value of the surfactant increases with the increment of linear alkyl chain length. Thus, there is an effect of alkyl side chain group lengths on the hydrophobicity of the surfactants. An increasing EO number enhances the hydrophilicity of the surfactant, while an increasing of alkyl chain length enhances its hydrophobicity.

The solubility of the prepared surfactants depends on the method of purification. However, there are some other means of minimizing the Gibbs function in our systems. Distortion of the solvent structure can also be diminished (and the Gibbs function of the solution reduced) by aggregation of the surface-active molecules into clusters (micelles) while their hydrophilic groups are directed towards the solvent. Micellization is therefore an alternative mechanism for adsorption at the interfaces for removing the lipophobic groups from contact with the solvent, thereby reducing the Gibbs function of the system.

The micellization and adsorption of surfactants are based on the critical micelle concentration c_{mc} which was determined by the surface balance method. To study the activity of the prepared surfactants at the water air interface, the surface tension γ as a function of the surfactant concentration in aqueous solution was measured using the du Nougy ring method. The c_{mc} values were determined at 25 °C from the changes in the slope of the plotted diagrams of surface tension γ *versus* the logarithmic solute concentration (ln *c*).

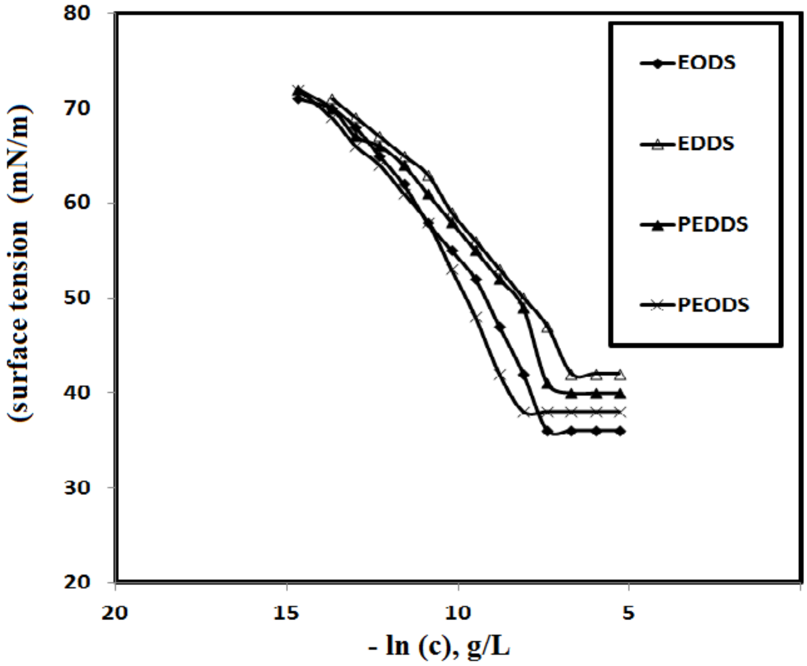

Figure 3. Adsorption isotherm of the prepared Schiff base surfactants at 25 °C.

These relations are illustrated in Figure 3. Values of c_{mc} at several temperatures are listed in Table 4. We see that the surface tension values increase upon decreasing the concentration of the surfactants. In our systemc c_{mc} values are affected by polymerization of Schiff base monomers and by alkyl chain lengths but are not significantly affected by variation of ethylene oxide unit lengths. This can be attributed to an increase of hydrophobic interaction between hydrophobic groups and an increase of intramolecular hydrogen bonding between hydrophilic groups – rather than by hydrogen bonds between water and hydrophilic groups of the modified surfactants.

When comparing the performance of different surfactants at interfaces, as in other similar situations, we need to distinguish between the amount of surfactant required to produce a given amount of change in the phenomenon under investigation and the maximum change in the phenomenon that the surfactant can produce, regardless of the amount used. The former parameter is the efficiency of the surfactant and the latter is its effectiveness. These two parameters do not necessarily run in parallel to each other when dealing with surfactants. The direct determination of the amount of surfactant adsorbed per unit area of liquid–gas or liquid–liquid interface, although possible, is not generally undertaken because of the difficulty of isolating the interfacial region from the bulk phase for purposes of analysis when the interfacial region is small, and of measuring the interfacial area when it is large. Instead, the amount of material adsorbed per unit area of interface is calculated indirectly from the surface or interfacial tension measurements. The concentration of surfactants at the water–air interface can be calculated as excess surface concentration $\Gamma_{\max}$. The variation of the surface tension as a function of the concentration leads to determination of the mass of the surfactant adsorbed at the surface, through the Gibbs adsorption isotherm [39], namely

$$\Gamma_{\max} = (-\partial \gamma / \partial \ln c)_T / RT \qquad (4)$$

Here $(-\partial\gamma / \partial \ln c)_T$ is the slope of the plot of γ *versus* ln c at a constant temperature T and R is the gas constant in the usual units (J mol^{-1} K^{-1}). The excess surface concentration at surface saturation is a useful measure of the effectiveness of adsorption of surfactant at the liquid–gas or liquid–liquid interface. The area per molecule at the interface provides information on the degree of packing and the orientation of the adsorbed surfactant molecules, when compared with the dimensions of the molecule as obtained from models.

From the surface excess concentration, the area per molecule at the interface is

$$A_{\min} = 10^{16} / N\,\Gamma_{\max} \qquad (5)$$

where N is the Avogadro number. The values of both $A_{\min}$ and $\Gamma_{\max}$ are also listed in Table 4.

The results show that the EPODS and EODS take up the smallest areas at the water/air interface (Table 4). This behavior can be attributed to tighter packing of the molecules of these surfactants at the interface [40]. The area occupied by the molecule of EPODS (0.75 nm^2/ molecule) is similar to that for the molecule of EODS (0.79 nm^2/molecule), even though the molar mass of EPODS is 11 times that of EODS (Table 3). A possible explanation: surfactant molecules tend to be adsorbed at the interface with a nonpolar segment turned away from the aqueous solution, while the polar segment is inside the solution. In the case of adjacent EPODS, the position of the molecule at the interface makes each of its three branches behave like an individual molecule [41].

The area taken up by a molecule of EPDDS at the surface of the aqueous solution was much greater than the areas found for the other EPODS. EPDDS has relatively low EO content and shorter lengths, factors which contribute to increase this value; it was observed that the surface of the aqueous solution was still not completely saturated [41]. The $A_{\min}$ and $\Gamma_{\max}$ results indicate the dependence of the effectiveness of adsorption at the aqueous solution–air interfaces on the structures of the surfactants. The nature of the hydrophilic groups has a major effect on the effectiveness of adsorption. In general, $A_{\min}$ appears to be determined by the cross-sectional area of the hydrated hydrophilic group at the interface. We find that the adsorption of the prepared surfactants at the water/air interface can be ordered as EPODS > EODS > EPDDS > EDDS.

3.3. Interfacial tension results

As said in Section 2.3, measurements of the water-petroleum interfacial tension (IFT) were performed using the pendant drop method. One can follow the variation of IFT values as a function of time. This, in turn, enables us to obtain these values after the system has reached equilibrium - when processes of diffusion, adsorption, reorganization at the interface, desorption, and transfer of the molecular mass to the other phase have taken place. Reaching the minimum interfacial tension value sooner means quicker diffusion of the molecules to the interface, leading to the formation of thinner and less elastic films that rupture more readily [42].

Our Schiff base monomers and polymers were dissolved in a mixture of xylene + ethanol (75:25) and then added to the petroleum phase at concentrations from 50 to 250 ppm. The IFT results are listed in Table 5. The variation of IFT data with time indicate that all of the Schiff base surfactants reduce the interfacial tension. At first, the interfacial tension values decrease with time, indicating that the molecules of the surfactants gradually migrate to the interface. EPODS and EODS are the most effective at reducing IFT; the droplets ruptured after 10 minutes. This behavior is related to the ability of these molecules to adsorb strongly at the interface – what enahnces the diffusion in the petroleum phase.

Table 5. IFT results for interfaces between different Schiff base aqueous surfactant solutions and crude petroleum at 25 ^{o}C.

Surfactants	Concentrations ppm	IFT (mN/m)		
		xylene/ethanol (75:25)	toluene	water
EODS	0	28	28	28
	50	22	25	26
	100	16	20	22
	250	6.3	8.2	14
EDDS	50	24	26	26
	100	18	20	22
	250	12	14	16
EPODS	50	16	18	20
	100	8	12	16
	250	2.6	6.5	10
EPDDS	50	18	20	22
	100	14	18	19
	250	8	12	14

In the case of the organic solvents, the surfactant was dissolved in the solvent and added to the petroleum, forming the interface with the water. In the case of the water used as the solvent for the co-polymer, this solution was added to the water that forms the interface with the petroleum. When the aqueous surfactant solution was added to the water phase, there was a greater reduction in interfacial tension after 25 min. This result reflects the high hydrophobicity of these surfactants which tend to migrate quickly to the interface to minimize its contact with the water. The xylene/ethanol (75:25) mixture provided the fastest reduction of the interfacial tension, reaching a value of 2.5 mN/m after 8 min. In the remaining systems, the tension decreased more gradually, and even after the longest measurement time (25 min), the tension still appeared to be declining slightly. The IFT values obtained at the end of the test can be interpreted as representing the influence of the solvent medium of the surfactant on its ability to reduce interfacial tension. The effectiveness of these three media was, in decreasing order: xylene/ethanol (75:25) > toluene > water.

3.4. Performance of the surfactants in the bottle tests

Asphaltene content in crude oil depends on the origin location. For example, the Arab heavy crude oil have different asphaltene contents varying from 0.1 to 20 wt. %. Generally, asphaltene is insoluble in small molecular normal alkanes such as *n*-pentane and *n*-heptane but soluble in benzene. Among crude petroleum constituents, asphaltene has the highest molecular weight (from ≈ 900 to 3500) and the strongest polarity. The basic structure of asphaltene involves condensed aromatic rings as a core, linked with many naphthenic, aromatic rings in addition to naphthenic rings, which carry many chains of varying length. Asphaltene molecules also contain many groups of sulfur, nitrogen, oxygen, even many metal complexes of iron, nickel, and vanadium, etc. After a systematic study of the asphaltene structure, Yen et al. [42] proposed a more representative asphaltic micelle model of the aggregation: there are 3 - 5 aromatic pieces or particles which become asphaltic micelles as a result of the intermolecular hydrogen bonding and dipolar forces. It is well known that asphaltene can hinder separation of oil and water phases. Because asphaltene molecules in oil easily gather at the oil/water interface and undergo self-association, they form a rigid film at the interface. In addition to absorbing such solid objects as paraffin and clay, the interfacial film become rigid [43]. Thus, as a surface-active substance, asphaltene in petroleum produces a stable emulsion which hinders the water separation. The higher the asphaltic content in the crude petroleum, the higher is the crude viscosity. The reason is that asphaltene forms associates in crude oil while it disperses as micelles at temperatures higher than 60 °C [44]. The viscosity increase, the asphaltene associate formation as well as accumulation of the micelles at the oil-water interface, not only resist the agglomeration of water drops, but also hinder the salt transfer from the oil phase to the aqueous phase. The result is a decrease of demulsification efficiency (DDE) of the surfactants.

We recall a value in Table 1: the Arab heavy crude oil has asphaltene contents 8.27 wt. %. Accordingly, there are two challenges in water separation from crude emulsions: the emulsion stability and demulsification, the latter particularly pronounced at temperatures below 45 ^{o}C.

The performance of the prepared surfactants in destabilizing the water-petroleum emulsions was evaluated by the bottle test. Several crude petroleum + formation water emulsions were prepared with the petroleum contents varying from 50 to 90 wt. Earlier work [15] the effect of the solvent on demulsification efficiencies in crude petroleum emulsions was investigated. It was found that xylene + ethanol mixtures have good demulsification efficiencies. As discussed by Lucas and her colleagues [45], aromatics have relatively higher solubility in water than aliphatics. For this reason and as noted in the previous section, xylene/ethanol (75:25) was selected. Several concentrations of our Schiff base surfactants were applied, from 50 to 250 ppm. The relation between DDE and time of water separation of EPODS was selected as representative and is plotted in Figures 4 and 5 for several crude petroleum + water emulsions and at temperatures 60 and 45 ^{o}C.

Table 6. DDE data of the surfactants at different concentrations and the separation temperature 60 °C.

Surfactants	conc. (ppm)	DDE %							
		O/W 90/10		O/W 80/20		O/W 70/30		O/W 50/50	
		DDE	Time (minute)	DDE	Time (minute)	DDE		DDE	Time (minute)
EODS	50	100	300	100	270	53	360	100	360
	100	100	90	100	180	60	360	100	90
	250	100	60	100	270	100	330	100	60
EDDS	50	80	360	100	300	67	360	100	240
	100	100	60	100	180	53	360	100	60
	250	100	45	100	330	100	330	100	90
EPODS	50	80	360	100	240	60	360	100	45
	100	100	60	100	90	100	45	100	45
	250	100	45	100	210	100	105	100	45
EPDDS	50	80	360	100	240	53	390	100	45
	100	100	90	100	90	100	90	100	45
	250	100	210	100	240	100	180	100	45

Table 7. DDE data of the surfactants at 250 ppm and the separation temperature = 45 °C.

Surfactants	conc. (ppm)	DDE %							
		O/W 90/10		O/W 80/20		O/W 70/30		O/W 50/50	
		DDE	Time (minutes)	DDE	Time (minutes)	DDE		DDE	Time (minutes)
EODS	250	100	420	100	330	33	480	88	480
EDDS	250	100	300	100	330	40	480	88	480
EPODS	250	100	180	100	240	80	480	100	45
EPDDS	250	100	240	100	300	67	480	100	45

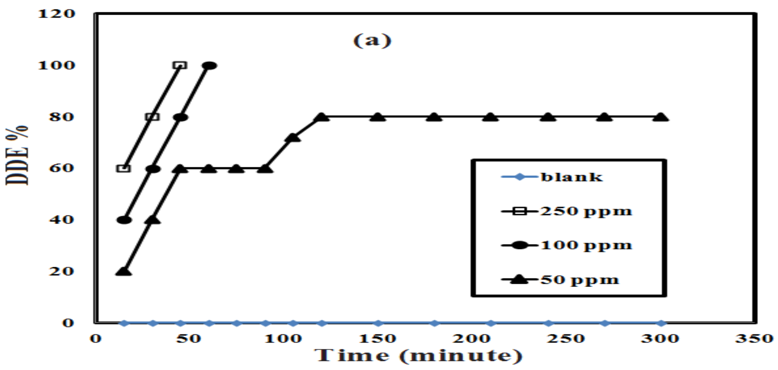

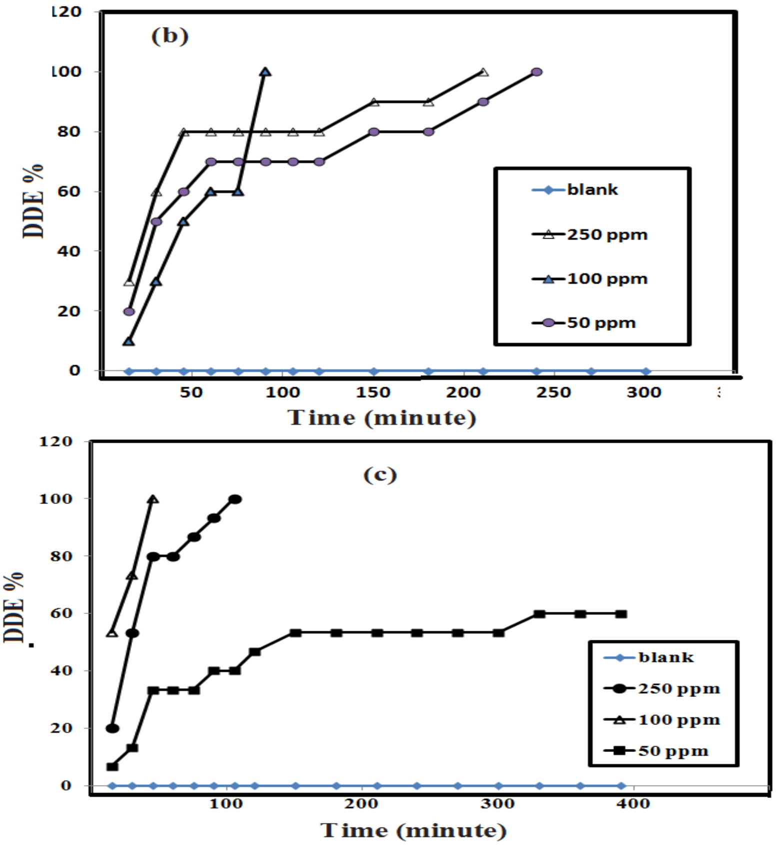

Figure 4. DDE of PEODS at different concentrations and separation temperature 60 °C for petroleum crude emulsions with different oil/water ratios: a) 90/10, b) 80/20 and c) 70/30.

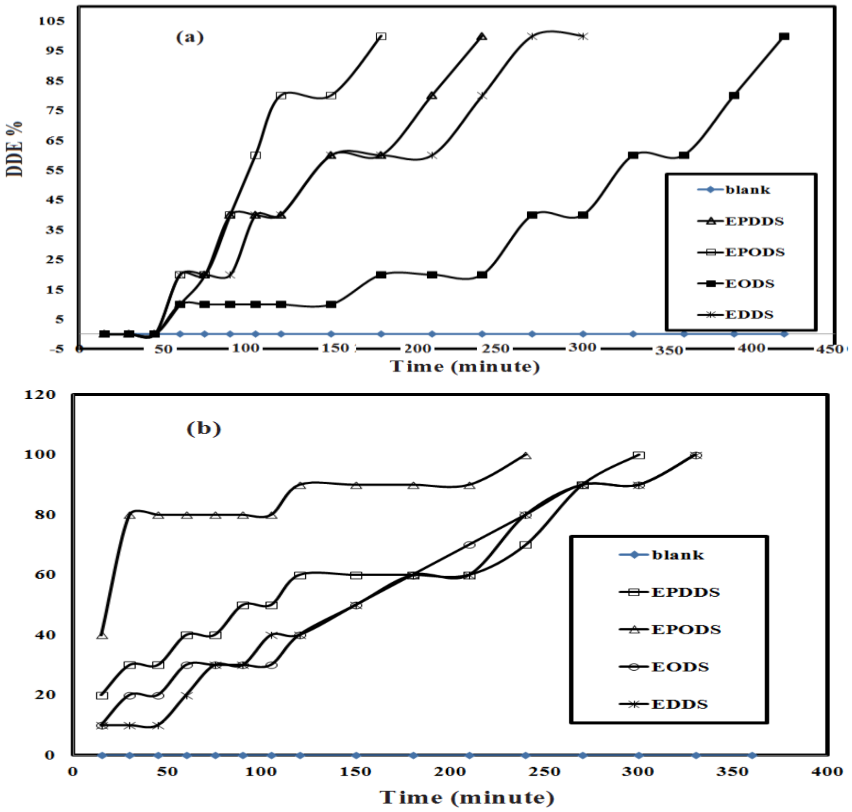

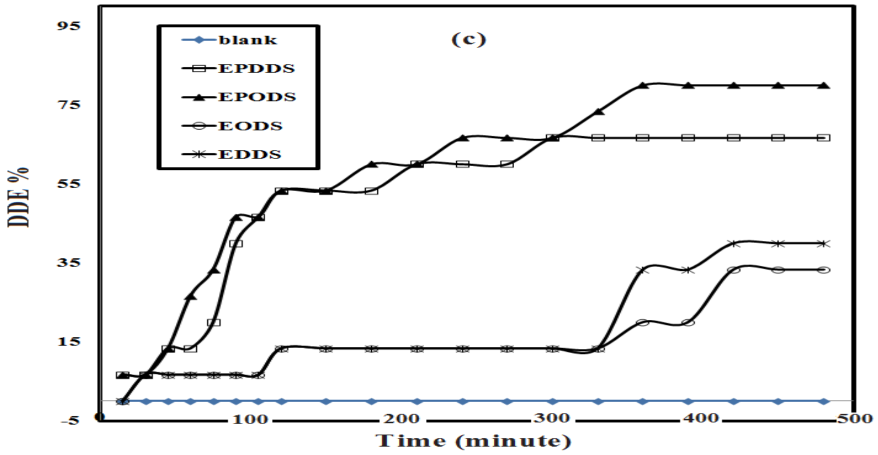

Figure 5. DDE of Schiff base surfactants at the concentration 250 ppm and separation temperature 45°C for petroleum crude emulsions with different oil/water compositions: a) 90/10, b) 80/20 and c) 70/30.

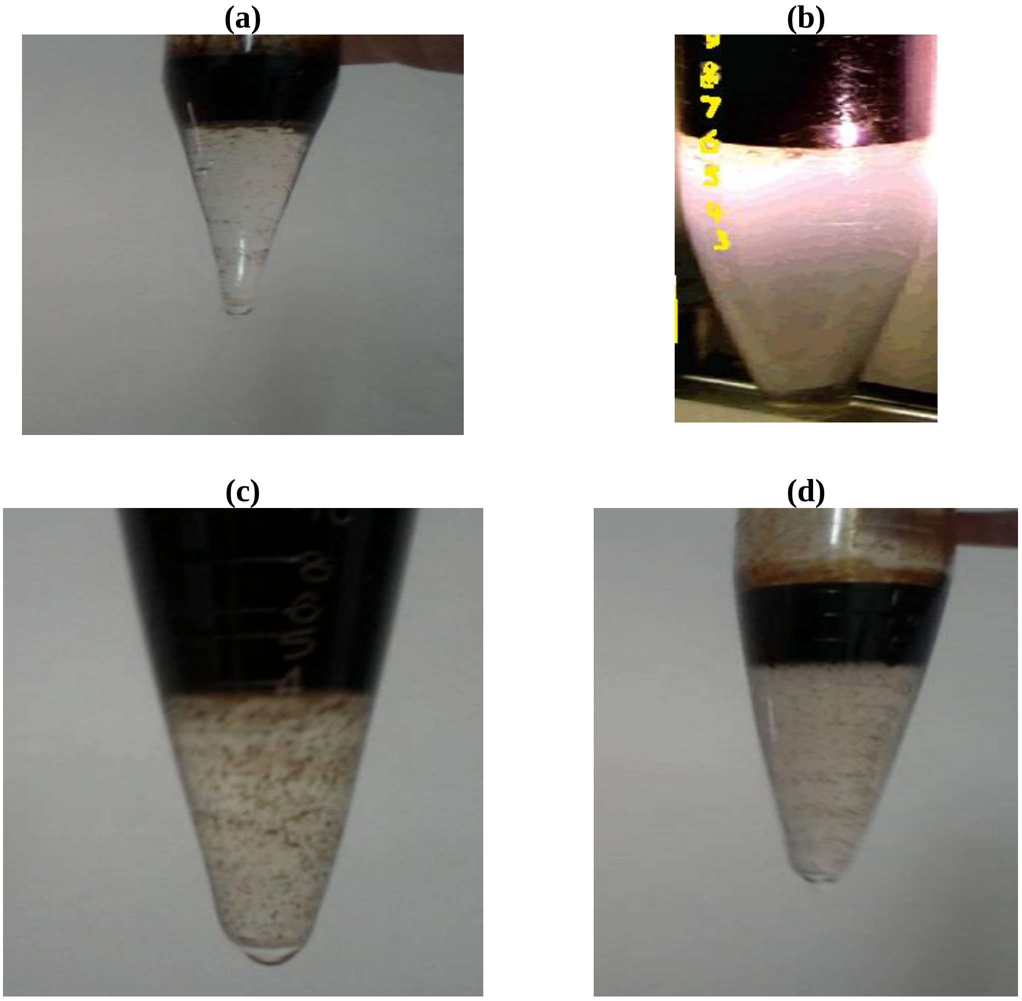

Figure 6. Photographs of water separation of crude oil emulsion 90/10 using 100 ppm of a) EODS, b) EPODS, c) EDDS and d) EPDDS surfactants.

The respective data are listed in Tables 6 and 7. Water separation from the emulsions after addition of Schiff base surfactants is represented in Figure 6.

We have observed that the emulsions changed color (becoming clearer), mainly when observed at the bottom of the tube used. This behavior appears to indicate the start of the droplet coalescence process, showing that these solvent media might be acting as co-additives in the demulsification process. Alcohols can also be acting as co-surfactants. The performance of a demulsifier is based on the interaction between dissolute surfactants and water droplets through diffusion and adsorption – what permits faster transport of demulsifier molecules to the water - droplet interface. Moreover, dissolved demulsifiers give a better separation of the phases than an undiluted demulsifier does. In general, Figures 4 and 5 show that there are steady states at which the dehydration rate remains constant for some time, and then it starts to increase again until reaching the final percentage of dehydration for each surfactant.

To understand this behavior, we have to consider more in detail the mechanism of demulsification. Crude oil emulsions are stabilized by surfactants, viz., asphaltenes and resins. The emulsions do not develop high surface pressures, therefore steric stabilization of water-in-crude-oil emulsions is the most plausible mechanism of the stabilization. Demulsifier molecules and natural surfactants compete with each other for adsorption onto the water-drop film. When demulsifier molecules - which lower interfacial tension much more than the natural surfactants - are adsorbed at the interface, the film becomes unstable in the direction of coalescence of water drops.

Emulsions formed in the petroleum industry are predominantly water-in-oil or regular emulsions, in which the oil is the continuous or external phase and the dispersed water droplets, form the dispersed or internal phase. The water droplets become bigger with time after demulsifier is added. The role of the demulsifier is to change the interfacial properties and to destabilize the surfactant-stabilized emulsion film in the demulsification process. In the beginning, there are small and uniform drops while larger drops begin to form after 30 min or so. Then two or more large drops continue to form a single larger drop: coalescence happens. The droplet size grows fast and the droplet number reduces after demulsifier is added. We concluded that coalescence of water droplets destroyed emulsions. Three terms related to stability commonly encountered in crude oil emulsion are “flocculation,” “coalescence,” and “breaking.” Although they are sometimes used almost interchangeably, those terms are in fact quite distinct in meaning as far as the condition of an emulsion is concerned. “Flocculation” refers to the mutual attachment of individual emulsion drops to form flocs or loose assemblies. Flocculation can be, in many cases, a reversible process, overcome by the input of much less energy than was required in the original emulsification process. It should be noted that the word flocculation is also well established when dealing with consolidation of solid suspensions such that the solid phase gradually goes to the bottom [46, 47].

“Coalescence” refers to the joining of two or more drops to form a single drop of greater volume, but with smaller interfacial area. Although coalescence will result in significant microscopic changes in the condition of the dispersed phase, it may not immediately result in a macroscopically apparent alteration of the system. The “breaking” of an emulsion refers to a process in which gross separation of the two phases occurs. In such an event, the identity of individual drops is lost, along with the physical and chemical properties of the emulsion. Such a process obviously represents a true loss of stability in the emulsion. The kinetics of chemical demulsification is largely determined by the interaction of three main effects. These are: the displacement of the asphaltenic film from the oil water interface by the demulsifier; flocculation; and coalescence of water drops [43, 44].

We find that in all cases an increase in the concentration of the additive improves its performance in destabilizing the emulsion. EPODS is the most efficient additive in breaking down the emulsion (Figures 4 and 5). After 15 min at concentrations of 100 and 250 ppm, approximately 90 % of the water had separated out. Complete phase separation was achieved at a concentration of 50 ppm after 45 min. The phase separation was much less efficient for the other surfactants EDDS, EPDDS and EDOS.

In general, the efficiency of the gravitational separation for the samples tested increased in the following order: EDDS < EPDDS < EODS< EPODS. Although EPODS was the most efficient in reducing the interfacial tension and EDDS was the least efficient (Table 5), there was no direct relationship between the efficiencies of the additives and the gravitational separation. EPODS may have performed best because it has the highest bulk phase concentration. If so, for these polymer additives, those that are poorly soluble in the aqueous phase perform better than those that are soluble in both phases.

We find there is a relationship among the efficiency of the gravitational separation, the molecular architecture, and the area occupied at the interface. The gravitational separation efficiency increases as the area occupied per molecule at the interface declines (Table 4). The better efficiency of EPODS in relation to EDDS can be related to the tighter packing of the molecules of the former. The decrease in demulsification power at surfactant concentration far above c_{mc} may be related to the saturation of the bulk phase by micelles - what leads to a reduction in the availability of crude petroleum soluble in surfactant micelles. The high demulsification power of surfactants based on EPODS and EODS reflects the hydration of long hydrophilic groups into bulk phase which prevents the crude oil to penetrate into the exterior region of micelle and to arrive in their cores and solubilize there [48]. At the same time, the long hydrophilic chains reduce the hydrophobicity of the surfactant molecule; hence the solubilization efficiency is reduced [49]. This behavior can be correlated with the ability of surfactants to reduce surface tension at c_{mc}, that is γ_{cmc}. Table 3 indicates that the ability of surfactants based on EPODS and EODS to reduce γ_{cmc} is larger than that for those based on EDDS and EPDDS.

The dehydration rates reach 100% for all surfactants - indicating their high efficiency for treating crude petroleum emulsions.

Surfactants with the HLB values ranging from 12.5 to 13.7 give high demulsification efficiencies. We have seen the lowest hydration rates of these surfactants for 70:30 water/petroleum emulsions. Hirasaki and coworkers [46] reported that the crude oil water emulsions having oil % (70 % oil) can be converted from water/oil emulsions to oil/water emulsions. The emulsion phase inversion was attributed to increase salinity of brine water in the produced emulsions with increase of water contents up to 30 %. Apparently the aqueous phase of the initial emulsion is below optimum salinity and hence is an oil/water microemulsion. Accordingly, the separation of water from this emulsion is difficult.

We find that the amount of water separated after 24 hours expressed as a percentage of coalescence increases with an increase in the HLB. This finding may be explained in terms of the following factors:

- The increase in the HLB value increases the solubility of the surfactant in the aqueous phase (dispersed phase). When the demulsifier is initially introduced to the water-in-oil emulsion, it will be thermodynamically stable at the interface of the water droplets. Accordingly, the surfactants possessing high HLB migrate faster to the interface than those having low HLB. As a result of such enhanced migration toward the interface, the surfactant forms a continuous hydrophilic pathway between the dispersed water droplets. This leads to a rapture of the interfacial oil film surrounding the water droplets.
- Another point of view regarding the enhanced demulsification efficiency of the more hydrophilic surfactants is based on the stability of emulsions containing asphaltene. The higher HLB surfactants show higher demulsification efficiency.

HLB is determined using Eqs. (2) and (3) that relate the length of the water-soluble portion of the surfactant to the oil-soluble portion of the surfactant. A surfactant with HLB between 1 and 8 promotes the formation of water–in–oil emulsions while one with an HLB between 12 and 20 promotes the formation of oil-in-water emulsions. A surfactant with HLB between 8 and 12 may promote either type of behavior. We find that the surfactants with HLB between 12.5 and 13.7 show good demulsification efficiencies. The surfactants having HLB above 13.8 show low demulsification efficiencies. This behavior reflects the dependence of the demulsification power on the presence of surfactant molecules in the soluble form rather than as micelles [49]. This can be attributed to the solubilization of crude oil into the hydrophobic interior core of micelle [50]. The data listed in Tables 5 and 6 indicate the DDE was affected by the temperature of separation. The dehydration rate of the surfactants was tested at 45^{o}C for different crude oil emulsion compositions using 250 ppm of surfactants solutions. We have found that the DDE was reduced in 70:30 (oil:water) emulsions and the time of water separation increases in the other emulsions. Solubility of our surfactants is naturally a function of temperature. Good solubility of surfactants in the petroleum phase is related to the presence of aromatic moieties in the structures of the surfactants [45].

Visual observations of the aqueous phase after the bottle tests shows that, when the solvent medium used is water, a large amount of petroleum is trapped on the walls of the glass tube, indicating that this medium does not favor diffusion of the molecules of the additive in the petroleum phase. A similar behavior is also observed when toluene is used as the solvent.

3.5. Electric desalting and dewatering efficiency

In some cases, the dewatering efficiency for crude oil is better, but desalting is worse during the electric desalting and dewatering process. Here desalting efficiency was used as the results of electric desalting and dewatering. Desalting efficiency (%) = (So - Si)/So x100 (mg/L), in which

So represents initial salt content in crude, respectively, whereas Si represents salt after desalting. In this respect, emulsion of 90/10 (w/o) was treated with 250 ppm of EPODS and used to carry out the experiment, then the rate of dewatering vs desalting and dewatering efficiency (DDE) can be observed in Figure 7.

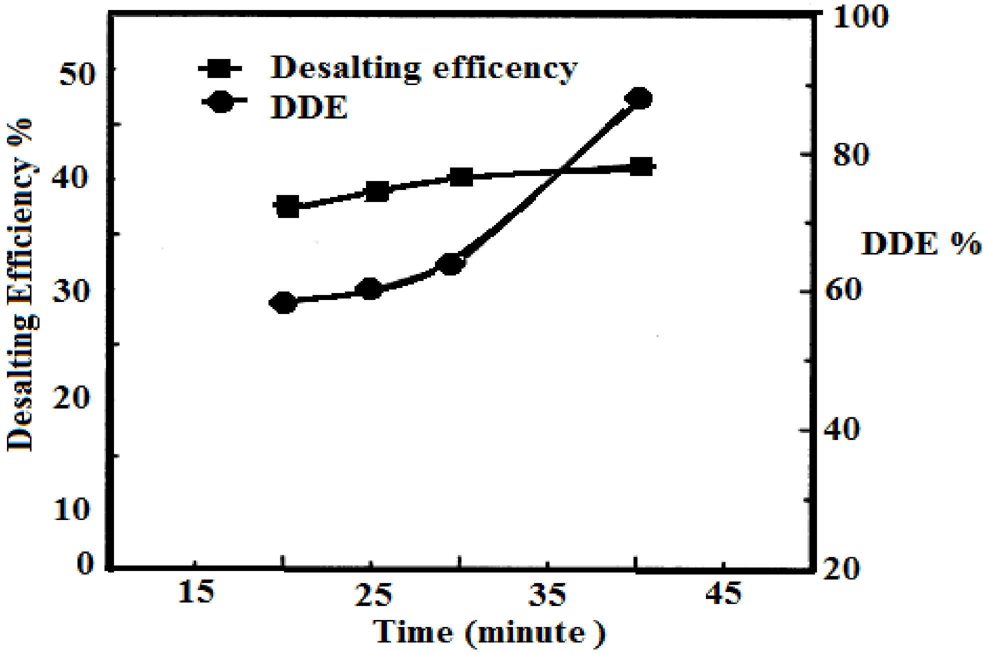

Figure 7. Electric demulsification and desalination rates versus separation time.

The desalting and dewatering efficiency are 45.2% and 70%, respectively, at 30 min settlement time, while dewatering efficiency reaches 80 % at 40 min settlement time, only 46.4% desalting efficiency, which is not as much as expected. This demonstrates that desalting efficiency is not in direct proportion to dewatering efficiency, namely, higher dewatering efficiency does not mean lower salt content in crude oil. The reason is that the desalting and dewatering process not only is a process of demulsification and settlement, but also includes oil-water mixing, washing, salt extracting, demulsifying, water-drop agglomerating, separating of water and oil, and so forth. This can be attributed to the high surface activity and high lipophilicity of EPODS will affect the stabilization of asphaltene colloid which increased the relatively rapid dewatering rate, but the salt transfer is a relatively slow process, that is to say, there exists a balance between desalting and dewatering efficiency in the electric desalting and dewatering process of crude oil, and the dewatering efficiency cannot match the dewatering efficiency when the requirement of the salt transfer from oil phase to aqueous phase cannot be met.

4. A SURVEY OF CONCLUSIONS

New water-soluble Schiff base surfactants have been prepared. The surface activity measurements indicate that increasing the length of hydrophobic saturated alkyl chain increases the surface excess concentration of molecules and consequently decreases A_{min} of molecules at the air-water interface. The adsorption of the surfactant molecules at that interface increases with increasing length of alkyl chain amines in the surfactants. Among our surfactant Schiff base polymers, the most efficient in promoting gravitational separation of water-in-oil emulsions was the polymer with adjacent polar and non polar segments. Efficiency of gravitational separation of synthetic emulsion of water-petroleum with the Schiff base surfactants solubilized in xylene/ethanol (75:25) and added to the emulsion at concentrations of 100 and 250 ppm show the best results for water separation. This result is due to the facility of the molecules of these polymers to diffuse into the petroleum phase of the emulsion and the action of the solvent used as a co-additive.

ACKNOWLEDGEMENTS
This project was funded by the Deanship of Scientific Research at King Saud University.

References

1. J. Eow, M. Ghadiri, *Chem. Eng. J. 85 (*2002) 357–368.
2. J. Wu, Y. Xu, T. Dabros, H. Hamza, *Energy Fuels 17* (2003) 1554-1559.
3. N. N.Zaki, N. E-S. Maysour, A. A. Abdel-Azim, *Pet. Sci. Technol. 18 (*2000) 1009-1025.
4. R. Aveyard, B. P.Binks, P. D. I. Fletcher, J. R. Lu, *J. Colloid Interface Sci. 139 (*1990) 128-138.
5. J. M. Williams, *Langmuir 7* (1991)1370-1377.
6. D. G. Cooper, J. E. Zajic, E. J. Cannel, J. W. Wood, *Can. J. Chem. Eng. 58 (*1980) 576-579.
7. J. C. Pereira, J. Delgado-Linares, C. Scorzza, M. Rondon, S. Rodríguez, J-L. Salager, *Energy Fuels 25 (*2011) 1045–1050.
8. D. Guzman-Lucero, P. Flores, T. Rojo, R. Martınez-Palou, *Energy Fuels 24 (*2010) 3610–3615.
9. M. A. Kelland, T. M. Svartås, L. D. Andersen, *J. Petr. Sci. Eng. 64 (*2009) 1-10.
10. M. Rondon, P. Bouriat, J. Lachaise, *Energy Fuels 20 (*2006) 1600-1604.
11. V.F. Pacheco, L.Spinelli, E. F. Lucas, C. R. E. Mansur, *Energy Fuels 25 (*2011) 1659–1666.
12. D.L. Marcell, R.A.Thatyana, M.D. Erika, C.S. Maria, M.S. Solange, L.W. James, F.F. Vitor, V.N. Marcus, *Carbohydr. Res. 12 (*2009) 2042-2047.
13. 13. J. Vancoa, O. Svajlenova, E. Racanskac, J. Muselika, J. Valentova, *J. Trace Elem. Med. Biol. 18 (*2004) 155- 161.
14. A.M. Atta, A.H.Abdel-Rahman, S.M.Elsaeed, S.Abou-Elfatouh, N.A. Hamad, *J. Disp. Sci. Technol. 29 (*2008) 1484-1495.
15. A.M. Atta, A.H. Abdel-Rahman, N.A. Hamad, *J. Disp. Sci. Technol. 29 (*2008) 1222-1232.
16. M.A. Migahed, A.A. Farag, S.M. Elsaed, R. Kamal, M. Mostfa, H. Abd El-Bary, *Mater. Chem. Phys. 125 (*2011) 125-135.
17. I.A. Aiad, N.A. Negm, *J. surfact. Deterg. 12 (*2009) 313- 319.
18. T. Kaliyappan, S. Rajagopan, P. Kannan, *J. Appl. Polym. Sci. 91 (*2004) 494–500.
19. A. M. Atta, N.O. Shaker, N.E. Maysour, *Prog. Org. Coat. 56 (*2006) 100–110.
20. M. H. Ese, X. Yang, J. Sjoblom, *Colloid Polym. Sci. 276 (*1998) 800-805.
21. A. Kopczynska, G.W. Ehrenstein, *J. Mater. Ed. 29 (*2007) 325-340.
22. R. J. Hunter, Foundations of Colloid Science; Clarendon Press: Oxford, U.K. (1986) 55-76.
23. Y. Saegusa, K. Sekiba, S. Nakamura, *J. Polym. Sci. Part A: Polym. Chem. 28 (*1990) 3647-3659.
24. Y. Saegusa, T. Koshikawa, S. Nakamura, *J. Polym. Part A: Sci. Polym. Chem. 30 (*1992) 1369-1373.
25. Y. Saegusa, T. Takashima, S. Nakamura, *J. Polym. Sci. Part A: Polym. Chem. 30(*1992) 1373-1381.
26. P. W. Margon, S. L. Guthrie, T. C. Pletcher, *Macromolecules 20 (*1987) 729-734.
27. P. W. Wojtkonski, *Macromolecules 20 (*1987) 740-745.

28. C. R. E. Mansur, C. M. F. Oliveira, G. Gonzalez, E. F. Lucas, *J. Appl. Polym. Sci. 66 (*1997) 1767–1772.
29. K. E. Arnold, H. V. Smith, Crude oil emulsions. In Petroleum Engineering Handbook, 3rd ed.; Bradley, H. B., Ed.; Society of Petroleum Engineers: Richardson, TX (1992) Chapter 19.
30. C. R. E. Mansur, S. P. Barboza, G. Gonzalez, E. F. Lucas, *J. Colloid Interface Sci. 271 (*2004) 232–238.
31. R. J. Hunter, Foundations of Colloid Science; Clarendon Press: Oxford, U.K. (1986) 22-33.
32. M. Razi, M. R. Rahimpour, A. Jahanmiri, F. Azad, *J. Chem. Eng. Data 56 (*2011) 2936–2945.
33. J. Wu, Y. Xu, T. Dabros, H. Hamza, *Colloids Surf. A 252 (*2005) 79–85.
34. W. D. Hergeth, I. Alig, J. Lange, J. R. Lochmann, T. Scherzer, S. Wartewig, *Makromol. Chem. Macromol. Symp. 52 (*1991) 289–296.
35. G. B. Roy, *Inorg. Chim. Acta 362 (*2009) 1709–1714.
36. K. Huang, B.P. Lee, D. R. Ingram, P. B. Messersmith, *Biomacromolecules 3 (*2002) 397-406.
37. D.K.Lee, J-Y. Choi, E. S. Lee, C-S. Ha, M. Han, J-Y. Bae, *J. Appl. Polym. Sci. 104 (*2007) 162–170.
38. W.C. Griffin, *J. Soc. Cosmet. Chem. 5 (*1954) 249-256.
39. Y. Xu, J. Wu, T. Dabros, H. Hamza, *Energy Fuels 19 (*2005) 916-921.
40. P. R. S. Silva, A. C.Mauro, C. R. E. Mansur, *J. Appl. Polym. Sci. 113 (*2009) 392–399.
41. E. F. Lucas, C. M. F. Oliveira, A. S. Gomes, _ *J. Appl. Polym. Sci. 46 (*1992) 733–737.
42. T. F. Yen, *Energy Sources 1 (*1974) 447-463.
43. Y.H. Kim, D. T. Wasan, *Ind. Eng. Chem. Res. 35 (*1996) 1141-1149.
44. C. M. Carmen, L. Carbognani, *Energy Fuels 15 (*2001) 1021-1027.
45. E.F. Lucas, C.R.E. Mansur, L. Spinelli, Y.G.C. Queirós, *Pure Appl. Chem. 81 (*2009) 473-494.
46. W. Brostow, S. Pal, R.P. Singh, *Mater. Letters 61 (*2007) 4381-4386.
47. W. Brostow, H.E. Hagg Lobland, S. Pal, R.P. Singh, *J. Mater. Ed. 31(*2009) 157-163.
48. M.J. Rosen, Surfactants and Interfacial Phenomena; New York: John Wiley and Sons. (1978) 53-68.
49. M.A. Cowell, T.C.G. Kibbey, J.B. Zimmerman, K.F. Hayes, Properties, *Environ. Sci. Technol. 34 (*2000) 1583-1588.
50. G. J. Hirasaki, C. A. Miller, O. G. Raney, M .K. Poindexter, D. T. Nguyen, J. Hera, *Energy Fuels 25 (*2011) 555–561.